Agricultural and Forest Meteorology 268 (2019) 124–135

Contents lists available at ScienceDirect

Agricultural and Forest Meteorology

journal homepage: www.elsevier.com/locate/agrformet

A new process-based model for predicting autumn phenology: How is leaf senescence controlled by photoperiod and temperature coupling?

Weiguang Lang, Xiaoqiu Chen*, Siwei Qian, Guohua Liu, Shilong Piao

College of Urban and Environmental Sciences, Laboratory for Earth Surface Processes of the Ministry of Education, Peking University, Beijing, China

ARTICLE INFO

Keywords:
Climate change
Plant phenology
Process-based leaf senescence model
Spatial and interspecific differentiation of driving factors
Model comparison
The Qinghai–Tibetan plateau

ABSTRACT

Autumn phenological variation of temperate and northern ecosystems plays a major but poorly defined role in the global carbon cycle. Constructing robust process-based autumn phenology models is key for improving current ecosystem models to accurately simulate ecosystem productivity and carbon sequestration. In this study, we developed a new process-based autumn phenology model. The model was fitted and validated using 67 leaf coloration and brown-down time series collected for 27 woody and herbaceous species at 18 stations on the Qinghai–Tibetan Plateau from 1981 to 2012. Then, we used the model to analyze the spatial and interspecific differentiation of driving factors of leaf senescence. Moreover, we compared fitting and validation precisions of the new model and previously published models. Results show that leaf senescence processes were triggered by photoperiod shortening in 61.2% of time series but by daily minimum temperature decrease in 38.8% of time series. Photoperiod control of the leaf senescence start occurs predominantly at stations with shorter annual maximum daylength (88.9%), while daily minimum temperature control of the leaf senescence start appears mainly at stations with longer annual maximum daylength (71.0%), especially for the native species. The new model reveals coupling effects of shortened photoperiod and decreased daily minimum temperature on leaf senescence processes. Comparing with the representative existing process-based autumn phenology models, the new model is a more general model and more robust in fitting and predicting leaf coloration and brown-down dates. Our study has provided a new insight on the understanding of leaf senescence mechanisms in winter deciduous trees and herbaceous plants, and significantly improved the ability to predict climate change impacts on vegetation growth and carbon balance in the sensitive biogeographical region of global climate change.

1. Introduction

Plant phenology is the study of the timing of annually recurring plant growth and reproductive phenomena, as well as the drivers of these events associated with endogenous and exogenous forces (Chen, 2017). Plant phenological variation has become a matter of global concern because the vegetation growing season defined by leaf unfolding date in spring and the leaf coloration date in autumn can serve as a key link between interactions of climate change and biogeochemical cycles (Keeling et al., 1996; Richardson et al., 2013; Chen, 2017). As the vegetation growing season is approximately equivalent to the photosynthetic period, carbon-uptake period, and transpiration period (Barr et al., 2009), climate change induced vegetation growing season shifts may influence the exchange capacities of carbon, water, and energy among land surfaces and the atmosphere, and consequently result in ecosystem productivity variations (Goulden et al., 1996; Myneni et al., 1997; Black et al., 2000; Wilson and Baldocchi, 2000; White and Nemani, 2003; Barr et al., 2004; Churkina et al., 2005; Kljun et al., 2007; Baldocchi and Wong, 2008; Delpierre et al., 2009a). Meanwhile, the exchange capacities of carbon, water, and energy in turn will affect the global carbon balance and climate change (Keeling et al., 1996; Schwartz, 1996; Peñuelas et al., 2009). Therefore, modeling growing season start and end dates is crucial for improving phenological modules in ecosystem models and enhancing their simulation and prediction accuracy of ecosystem productivity in a context of climate change (Baldocchi and Wilson, 2001; Dufrêne et al., 2005; Richardson et al., 2013).

So far, process-based spring plant phenology model has reached maturity. Scientists developed numerous temperature and precipitation based models to simulate and predict budburst, green-up, leafing and flowering dates (Vegis, 1964; Landsberg, 1974; Kobayashi et al., 1982; Cannell and Smith, 1983; Murray et al., 1989; Hänninen, 1990; Kramer, 1994; Chuine et al., 1998; Chuine, 2000; Linkosalo et al., 2008; Morin et al., 2009; Richardson and O'Keefe, 2009; Fu et al., 2012; Chen et al.,

* Corresponding author: College of Urban and Environmental Sciences, Peking University, Beijing 100871, China.
E-mail address: cxq@pku.edu.cn (X. Chen).

https://doi.org/10.1016/j.agrformet.2019.01.006
Received 10 August 2018; Received in revised form 3 January 2019; Accepted 4 January 2019
Available online 18 January 2019
0168-1923/

2015). By contrast, studies on process-based autumn plant phenology model are still scarce. Main reasons for this are inadequate ground observation data and unclear environmental cues of autumn phenology. Statistical studies showed that changes in autumn leaf phenology in temperate forests can better explain variation in annual net ecosystem productivity (NEP) than do changes in spring phenology (Wu et al., 2013), and delayed autumn leaf senescence is associated with increased NEP, meaning that ecosystems tend to sequester more carbon in warmer years with later autumn phenology (Hollinger et al., 2004; Richardson et al., 2010; Dragoni et al., 2011; Keenan et al., 2014). Thus, autumn leaf phenology plays a very important role in ecosystem functioning. The lag in developing process-based autumn phenology models comparing with process-based spring phenology models has become a bottleneck in predicting ecosystem productivity and carbon assimilation.

From the viewpoint of plant physiology, there is a general consensus that leaf senescence is controlled by photoperiod and temperature (Delpierre et al., 2009b; Fracheboud, et al., 2009). As photoperiod shortens and temperature decreases in late autumn, an abscission zone starts to form at the base of the petiole (Worrall, 1998) and chlorophyll degradation occurs (Addicott, 1968; Koike, 1990; Rosenthal and Camm, 1996; Fracheboud, et al., 2009; Archetti, et al., 2013). Multiyear observations and experiments suggest a strong photoperiodic regulation of leaf senescence at latitudes with severe winters (Barr et al., 2004; Fracheboud et al., 2009; Soolanayakanahally et al., 2013). At lower latitudes where winters are less severe, temperature exerts a certain amount of control on autumn phenology (Pudas et al., 2008). How the control of leaf senescence is split between photoperiod and temperature, however, is not known for many species (Estiarte and Peñuelas, 2015).

Regarding existing process-based autumn phenology models, Dufrêne et al. (2005) first proposed a cold-degree day sum (CDD) model and embedded it in a forest ecosystem model. The CDD model assumes that leaf coloration is solely determined by linear accumulation of daily mean temperature lower than a threshold, but its simulation accuracy has not been assessed. Then, Delpierre et al. (2009b) postulated that leaf coloration is driven by both photoperiod and low temperatures and revised the CDD model by means of a photoperiod-sensitive cold-degree day summation procedure (termed the DM model). In the DM model, only when both photoperiod and temperature reach their thresholds respectively, the leaf senescence process can start. The leaf senescence rate is determined by daily mean temperature lower than the threshold and a photoperiod function. In addition, two dummy parameters x and y were used as power exponents of the temperature difference and photoperiod function to regulate the daily leaf senescence rate. Spatiotemporal series fitting of leaf coloration date shows that leaf senescence rate for *Fagus* was affected by both temperature and photoperiod, but for *Quercus* was affected only by temperature. When the DM model was used to fit 50% leaf coloration date at different elevations in southwestern France, the selected best model structure for 2 of 3 species did not incorporate an interaction effect of photoperiod and cold-degree-days (Vitasse et al., 2011). Similar results were also obtained by a leaf coloration modeling study in China. Specifically, leaf coloration in 2 of 3 species was driven only by temperature (Tao et al., 2017). The above studies indicate that the photoperiodic impact on leaf senescence is not always effective in the DM model. Based on positive correlation between autumn senescence timing and spring budburst timing in Europe (Fu et al., 2014) and eastern United States, Keenan and Richardson (2015) modified the DM model by means of a linear regression equation between spring budburst date and the threshold value of senescence state and termed the Spring Influenced Autumn Model (SIAM). The SIAM puts more empirical components into the process-based model.

In light of this, we attempted to develop a new process-based autumn phenology model to portray coupling controls of photoperiod and temperature on leaf senescence process and simulate autumn leaf phenology. As the recent warming rate of the Qinghai–Tibetan Plateau has been greater than those for the northern and southern hemispheres, and the world as a whole (IPCC, 2013), the world's highest plateau has become a sensitive region of global climate change (Chen et al., 2013). Thus, predicting autumn plant phenology on the Qinghai–Tibetan Plateau takes on particular importance for providing early signals of climate change impacts on vegetation growth and carbon balance. We selected the Qinghai–Tibetan Plateau as our research region to address following scientific questions: (1) How do photoperiod and low temperature interact to control leaf senescence process? (2) Do effects of photoperiod and low temperature on inducing leaf senescence have specific spatial patterns and species dependence? and (3) Whether the new process-based autumn phenology model has higher accuracy, reality and generality than previous models?

2. Materials and methods

2.1. Study area

The Qinghai–Tibetan Plateau in western and southwestern China is the highest plateau in the world and the largest plateau in China, embracing an area of approximate 2.5 million km^2 at an average elevation of 4000 m. Surrounded by many massive mountains exceeding 6000 m above mean sea level (a.m.s.l), it forms a unique biogeographical region. Our study area is located in the eastern and southeastern parts of the Qinghai–Tibetan Plateau, which contains two climate zones (plateau temperate zone and plateau sub-cold zone) and six climate regions (temperate humid, sub-humid, semi-arid and arid regions, and sub-cold humid and sub-humid regions) (Fig. 1; Zheng et al., 2015). The annual mean air temperatures range from -1.7 °C to 9.2 °C, while the annual mean total precipitations are between 51.1 mm and 686.2 mm during 1981–2012. Regarding seasonal variations, the daily mean temperatures from midsummer (15 July) to autumn (30 November) drop from 20.7 °C to -2.2 °C at the lowest elevation site (Minhe, Table 1) and from 9.3 °C to -9.8 °C at the highest elevation site (Shiqu, Table 1), while the daily minimum temperature during the same period decreases from 14.8 °C to -6.3 °C at Minhe (Table 1) and from 4.1 °C to -18.4 °C at Shiqu (Table 1). Moreover, the daily photoperiod declines from 14.0 h to 10.4 h at the southernmost site (Daocheng, Table 1) and from 14.7 h to 9.8 h at the northernmost site (Menyuan, Table 1) from 21 June (day of summer solstice) to 30 November. The vegetation types involved in this study include steppe, meadow, forest, shrub, desert, and cultivated vegetation (Editorial Board of Vegetation Map of China CAS, 2001).

2.2. Phenological and climatic data

Plant phenological data during 1981–2012 used in this study were acquired from the China Meteorological Administration (Chen, 2013). According to the observation criteria, autumn leaf phenology is identified by first leaf coloration, full leaf coloration, first leaf fall, and the end of leaf fall for woody plants, and first brown-down, common brown-down, and the end of brown-down for herbaceous plants. As first leaf coloration and common brown-down dates were more frequently recorded than full leaf coloration and first brown-down dates, we selected the first leaf coloration date of woody plants and the common brown-down date of herbaceous plants for modeling autumn phenology. For each species, three to five individual trees and ten individual grasses were selected as fixed observation objects. The first leaf coloration (LC) date is defined as the day when about 5% of canopy leaves turn from green to yellow or red on more than half of the observed trees, while the common brown-down (BD) date is identified as the day when more than 50% of basal green leaves turn to withered and yellow on more than half of the observed herbaceous plants. The species-specific phenological observations are carried out every 2 days by professionals according to uniform observation criteria (China Meteorological Administration, 1993). To assure an adequate spatial

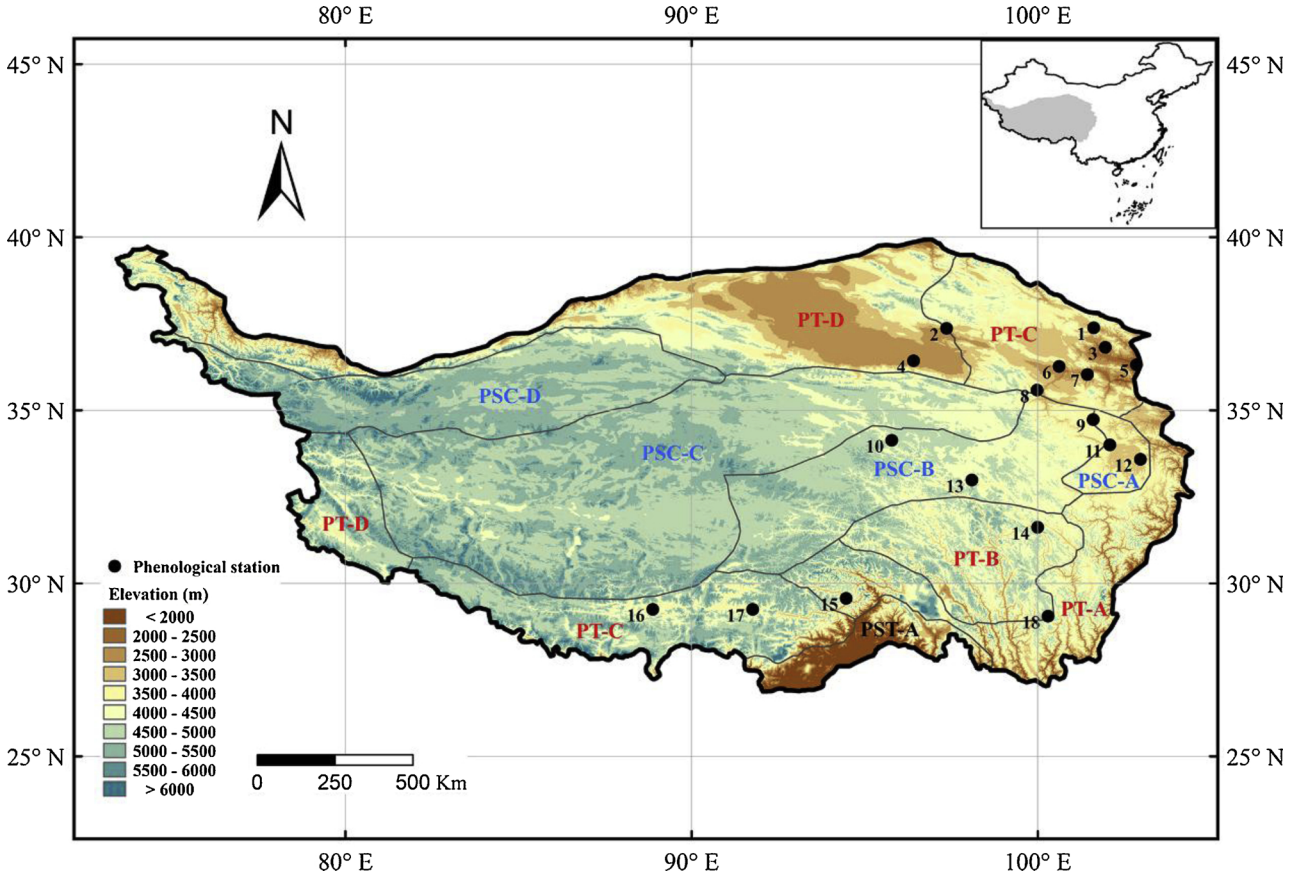

Fig. 1. Geographical distribution of phenological stations and climate regions on the Qinghai–Tibetan Plateau. PT, PSC and PST denote plateau temperate zone, plateau sub-cold zone and plateau sub-tropical zone, respectively. A, B, C and D represent humid, sub-humid, semi-arid and arid regions, respectively.

and species representativeness, we chose 67 time series from 27 species at 18 phenological stations with a time series length of at least 10 years for fitting autumn phenology models (Fig. 1 and Table A.1), which include 21 time series from 10 woody plant species (including *Amygdalus davidiana, Armeniaca vulgaris, Lycium chinense, Populus Canadensis, Populus lasiocarpa, Populus simonii, Salix cupularis, Salix matsudana, Tamarix ramosissima* and *Ulmus pumila*) and 46 time series from 17 herbaceous plant species (including *Agropyron cristatum, Carex przewalskii, Elymus nutans, Festuca ovina, Iris lacteal, Kobresia pygmaea, Koeleria cristata, Leymus secalinus, Medicago sativa, Phragmites australis,*

Table 1
Detailed information for each phenological station.

Station name	Station number	East longitude	North latitude	Elevation (a.m.s.l)	Annual mean temperature (°C)	Annual total precipitation (mm)	Vegetation type
Menyuan	1	101°37′	37°23′	2851.0	1.3	528.9	Cultivated vegetation
Delingca	2	97°22′	37°22′	2982.4	4.4	204.9	Desert
Huzhu	3	100°57′	36°49′	2480.8	6.1	399.3	Cultivated vegetation
Nuomuhong	4	96°25′	36°26′	2791.4	5.3	51.1	Cultivated vegetation
Minhe	5	102°51′	36°19′	1814.8	8.3	337.4	Steppe
Qabqa	6	100°37′	36°16′	2836.0	4.6	323.7	Desert
Guide	7	101°26′	36°02′	2238.1	7.6	255.6	Cultivated vegetation
Xinghai	8	99°59′	35°35′	3324.3	1.8	380.5	Steppe
Henan	9	100°36′	34°44′	3501.0	−0.2	569.8	Meadow
Qumarleb	10	95°47′	34°08′	4176.4	−1.7	429.0	Steppe
Maqu	11	102°05′	34°00′	3473.2	1.9	598.6	Steppe
Zoige	12	102°58′	33°35′	3441.1	1.5	648.0	Meadow
Shiqu	13	98°06′	32°59′	4201.0	−0.8	570.0	Meadow
Garze	14	100°00′	31°37′	3394.2	6.0	652.3	Cultivated vegetation
Nyingchi	15	94°28′	29°34′	3001.0	9.1	686.2	Forest
Shigatse	16	88°53′	29°15′	3837.0	9.2	381.4	Cultivated vegetation
Lhoka	17	91°46′	29°15′	3553.2	6.9	426.6	Shrub
Daocheng	18	100°18′	29°03′	3728.6	4.8	646.8	Meadow

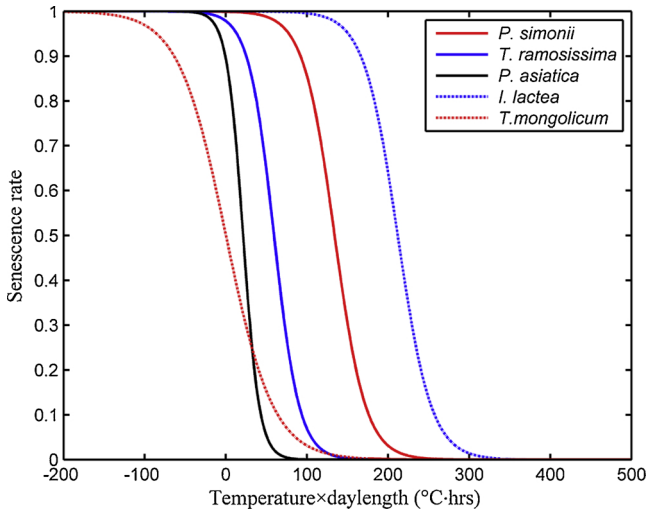

Fig. 2. Dependence of daily leaf senescence rate (R_{sen}) on the arithmetic product of daily minimum temperature and photoperiod, as fitted from observed leaf coloration and brown-down data for five plant species at Menyuan (station 1).

Plantago asiatica, Poa alpine, Poa annua, Puccinellia tenuiflora, Scirpus distigmaticus, Stipa sareptana and Taraxacum mongolicum). As each plant species has a different distribution range, the number of stations for autumn leaf phenology modeling is different for each plant species.

The station latitudes and longitudes range from 29°03′N to 37°23′N and from 88°53′E to 102°58′E, respectively, while the station elevations are between 1814.8 m and 4201 m. Detailed station names, geo-location parameters (latitude, longitude and elevation), mean annual air temperatures, mean annual total precipitations, and vegetation types are listed in Table 1.

Daily minimum air temperature and daily mean air temperature were used as climate drivers to create the new process-based model of leaf senescence in this study, and to fit existing process-based models of autumn phenology, respectively. Daily minimum and daily mean air temperature data at 18 national meteorological and climatological stations from 1981 to 2012 were acquired from China Meteorological Data Service Center (http://data.cma.cn/). These meteorological and climatological stations are all located at or nearby the corresponding phenological stations. The maximum distance between a phenological and a meteorological station is 5 km (Qabqa, Table 1). All temperature data were examined and verified by the China's Meteorological Information Center. Another climate driver of autumn leaf senescence is photoperiod. We employed the modified Schoolfield's equations (Forsythe et al., 1995) to calculate daily daylength (photoperiod) for each station based on latitudes and day of year (DOY).

2.3. Process-based autumn leaf phenology model

From the physiological and ecological perspectives, photoperiod controls the induction of leaf abscission meristems and freezing resistance, while temperature plays a modulating role and triggers the visible progress of phenology, such as leaf coloration in many species (Körner and Basler, 2010; Liu et al., 2018). Some studies showed that the photoperiodic control on the initiation of overwintering processes can be modulated by low temperature at varying intensities (Tanino et al., 2010). On the basis of these evidences, we proposed a new autumn leaf phenology model based on daily minimum temperature and photoperiod, the Low Temperature and Photoperiod Multiplicative Model (TPM). The basic hypothesis is that plant leaf senescence starts when either photoperiod or minimum temperature achieves a threshold and its status is controlled by the interaction of low temperature and photoperiod; as daily minimum temperature decreases and photoperiod shortens in autumn, the leaf senescence rate increases. When the leaf senescence state (S_{sen}) reaches the critical value (S^*_{sen}) on date Y, the autumn leaf phenology (LC/BD) will occur [Eq. (1)].

$$S_{sen} = \sum_{i=D_{start}}^{Y} R_{sen}(T_i, P_i) = S^*_{sen} \tag{1}$$

where the leaf senescence state (S_{sen}) is the sum of daily leaf senescence rate (R_{sen}) from D_{start} to the date when autumn leaf phenology (LC/BD) occurs (Y). D_{start} can be determined in two ways. If leaf senescence start is assumed to be triggered by photoperiod, D_{start} is defined as the first day when photoperiod is shorter than a photoperiod threshold (P_{start}) after the date of the longest photoperiod (summer solstice), namely, the 173rd day of year [Eq. (2)]. If leaf senescence start is assumed to be triggered by low temperature, D_{start} is defined as the first day when daily minimum temperature is lower than a temperature threshold (T_{start}) after the date of the peak multiyear average daily minimum temperature, namely the 200th day of year [Eq. (3)].

$$D_{start} = firstday \quad when \quad P_{i>173} < P_{start} \tag{2}$$

$$D_{start} = firstday \quad when \quad T_{i>200} < T_{start} \tag{3}$$

Daily leaf senescence rate (R_{sen}, arbitrary unit) is an exponential function of the arithmetic product of daily minimum temperature and photoperiod [Eq. (4)] and increases with the decrease of arithmetic product of minimum temperature and photoperiod (Fig. 2).

$$R_{sen}(T_i, P_i) = \begin{cases} 1/(1 + \exp(a \times (T_i \times P_i - b))) & i \geq D_{start} \\ 0 & i < D_{start} \end{cases} \tag{4}$$

where T_i is the minimum temperature in day i, while P_i is the photoperiod in day i. The autumn leaf phenology model contains four fitted parameters, P_{start}/T_{start}, a, b, and S^*_{sen}, with a > 0 and b > 0. The model induced by photoperiod (P_{start}) is abbreviated by TPMp, while the model induced by temperature (T_{start}) is abbreviated by TPMt.

In addition, to identify the relative role of daily minimum temperature and photoperiod on R_{sen}, we calculated the partial derivative of leaf senescence rate (R_{sen}) with respect to temperature (namely, the sensitivity of R_{sen} to temperature) and photoperiod (namely, the sensitivity of R_{sen} to photoperiod) within the multiyear range of daily minimum temperature and photoperiod for each species at each station, respectively.

2.4. Model parameterization and evaluation

The local species-specific models were evaluated based on two criteria: the root mean square error (RMSE) and the Nash-Sutcliffe Efficiency (NSE). First, the species-specific parameters of TPMp and TPMt at a station were determined by the lowest value of the RMSE [Eq. (5)] among different parameter combinations using the simulated annealing algorithm of Metropolis (Chuine et al., 1998). Second, the optimum local species-specific model was selected by the lower value of RMSE between TPMp and TPMt because the number of parameters of established species-specific TPMp and TPMt at a station is the same. Moreover, the NSE [Eq. (6)] (Nash and Sutcliffe, 1970) was used to assess simulation effectiveness of established optimum local species-specific model (TPMp or TPMt) by comparing with the null model (mean dates of leaf coloration/brown-down). A negative NSE value denotes that the model performs worse than the null model, whereas a positive NSE value (with a maximum value of 1) indicates that the model explains more variance than the null model. The closer the NSE value to 1, the higher the model effectiveness, whereas the closer the NSE value to 0, the lower the model effectiveness.

$$RMSE = \sqrt{\frac{\sum_{i=1}^{n}(obs_i - fit_i)^2}{n}} \tag{5}$$

$$NSE = 1 - \frac{\sum_{i=1}^{n}(obs_i - fit_i)^2}{\sum_{i=1}^{n}(obs_i - \overline{obs})^2} \quad (6)$$

where obs_i and fit_i are the observed and fitted autumn phenological date in year i, respectively; n is the number of years; $\overline{obs}$ is mean observed autumn phenological date during the study period. Moreover, the RMSE and AICc [Eq. (7)] (Hurvich and Tsai, 1989) were used to compare fitting accuracy among our new model (TPM) and previously published models (DM and SIAM; detailed description in Appendix B) over the 66 phenological time series (except for *Iris lactea* at Xinghai station due to lack of green-up data). AICc rates models in terms of parsimony and efficiency.

$$AICc = n \times \ln\left(\frac{\sum_{i=1}^{n}(obs_i - fit_i)^2}{n}\right) + \frac{2n(k+1)}{n-k-2} \quad (7)$$

where k is the number of parameters; the other variables are the same as in Eqs. (5) and (6).

2.5. Model validation

To evaluate the ability of the optimum models (TPMp or TPMt) in predicting leaf coloration and brown-down dates in years beyond the time period of model fitting, we conducted a leave-one-out cross-validation analysis (Hastie et al., 2001; Hagen et al., 2006). Specifically, each optimum local species-specific model was fitted sequentially on leaf coloration and brown-down dates of *n-1* years from the original time series ('calibration') and tested for their ability to simulate leaf coloration and brown-down dates of the remaining year ('validation'). This process was repeated n times, so that leaf coloration and brown-down dates of each year were included in the validation set exactly once. The RMSE was then calculated across the n validation years (Archetti et al., 2013). This cross-validation is particularly appropriate when the dataset is relatively small. In addition to assess the robustness of our new model (TPM), the leave-one-out cross-validation was also employed to compare the ability in predicting leaf coloration and brown-down dates in years beyond the time period of model fitting among TPM, DM and SIAM.

3. Results

3.1. Autumn leaf phenology modeling and validation

We fitted TPMp and TPMt using 67 autumn leaf phenological time series from 27 species at 18 phenological stations during 1981–2012 and selected the optimum models for each time series based on the smaller RMSE value. Results show that NSEs of all optimum models are larger than 0 with the average NSE of 0.25 for woody plants and 0.3 for herbaceous plants. Fitting errors (RMSE) range from 2.3 days to 21.1 days, and the average RMSE is 8.0 days. The percentage of optimum models with RMSE ≤ 10 days accounts for 80.6%. Considering the difference between woody and herbaceous plants, fitting errors for woody plant leaf coloration date range from 4.1 days to 18.9 days with the average RMSE of 8.2 days, whereas fitting errors for herbaceous plant brown-down date are between 2.3 days and 21.1 days with the average RMSE of 8.0 days. Percentages of optimum models with RMSE ≤ 10 days are 85.7% for woody plants and 78.3% for herbaceous plants, respectively. The correlation coefficients between fitted and observed autumn leaf phenology dates are significantly positive ($p < 0.05$) in 67.2% of all optimum local models, and in 76.2% of local woody plant models and in 63.0% of local herbaceous plant models (Table A1).

Moreover, we compared mean parameters (a, b, S^*_{sen}) and NSE, and their standard deviations (s) between woody and herbaceous plants (Table 2). Results show that either TPMp or TPMt does not show significant difference between woody and herbaceous plants in model parameters a, S^*_{sen} and NSE (Table 2). However, parameter b for woody plants is much larger than that for herbaceous plants in the two types of models, which indicates that leaf senescence process of woody plants occurs normally in higher temperatures and longer photoperiods (earlier timing) than that of herbaceous plants.

As the model selecting process determine the optimum model and associated D_{start} at the same time, we further analyzed differences in D_{start} between the optimum model and the corresponding non-optimum model for each species at each station. It should be noted that D_{start} in TPMp is a fixed date for a specific species at a given station but D_{start} in TPMt varies from year to year for a specific species at a given station. The results show that in the 41 time series with the optimum model TPMp, D_{start} in 31 time series (76% of total) is later than the average D_{start} in the non-optimum model TPMt (Fig. 3a, Table A.2). However, in the 26 time series with the optimum model TPMt, the average D_{start} only in 13 time series (50% of total) is later than D_{start} in the non-optimum model TPMp (Fig. 3b, Table A.2). Thus, the optimum model TPMp is characterized by predominant later D_{start} dates than the non-optimum model TPMt, while the optimum model TPMt and non-optimum model TPMp cannot be distinguished by D_{start} dates.

By comparing the average and the range of fitted senescence dates with that of observed senescence dates, the RMSE between fitted and observed senescence dates (LC/BD) are 1.0 days for woody species (Fig. 4a) and 0.7 days for herbaceous species (Fig. 4b), respectively. However, the range of fitted phenological dates, that represents interannual variability, is generally smaller than that of observed phenological dates. In 66.7% of time series of woody plants, observed senescence dates in more than 50% of years fall within the range of fitted senescence dates. By contrast, in 76.1% of time series of herbaceous plants, observed senescence dates in more than 50% of years fall within the range of fitted senescence dates. Thus, local species-specific TPM can effectively predict autumn phenology in normal years but cannot capture timing of autumn events during extreme years well.

Further leave-one-out cross-validation analysis indicates that validation errors (RMSE) of the 67 optimum local species-specific models range from 2.7 days to 25.1 days with the average RMSE of 10.7 days, which is 2.7 days larger than the fitting error on average. For woody plants, validation RMSEs range from 4.7 days to 21.9 days with the average value of 10.1 days, whereas for herbaceous plants, validation RMSEs are between 2.7 days and 25.1 days with the average value of 11.0 days. The average validation RMSEs are 1.9 days and 3.0 days larger than the average fitting RMSEs for woody and herbaceous plants, respectively.

3.2. Spatial and interspecific differentiation of driving factors of leaf senescence

From the perspective of the driving factors of leaf senescence, TPMp was identified as the optimum model in 61.2% of the local species-specific fitting, indicating that leaf senescence processes were predominantly initiated by photoperiod shortening. For the other 38.8% of optimum models in the form of TPMt, leaf senescence processes were induced by daily minimum temperature decrease. Regarding woody and herbaceous plants, the percentages of TPMp and TPMt are similar, namely, 61.9% and 38.1% for woody plants and 60.9% and 39.1% for herbaceous plants (Table A.1).

To identify spatial and interspecific differentiation of the driving factors of leaf senescence, we arranged the 67 optimum models of 27 species from 18 stations in accordance with type of the species (y-axis of Fig. 5) and ascending order of annual maximum daylength (photoperiod) of the stations (x-axis of Fig. 5). Results show that climatic controls on the start of leaf senescence processes are generally location-specific, namely, the optimum models have the same form (TPMp or TPMt) at 9 stations (18 stations in total, accounting for 50%) and a dominant form (TPMp dominance or TPMt dominance) at 8 stations (18 stations in total, accounting for 44.4%) regardless of plant species.

Table 2
Differences in average model parameters (a, b, S^*_{sen}) and NSE and their standard deviations (s) of TPMp and TPMt in woody and herbaceous plants.

Optimum model	Plant species	$a \pm s$	$b \pm s$	$S^*_{sen} \pm s$	NSE ± s
TPMp	Woody plant	0.057±0.033	129.64±74.63	32±35.05	0.23±0.16
	Herbaceous plant	0.065±0.034	79.51±61.05	33.93±24.06	0.31±0.2
TPMt	Woody plant	0.042±0.037	158.43±68.23	32.72±15.91	0.29±0.09
	Herbaceous plant	0.048±0.038	120.04±72.64	35.36±18.77	0.27±0.13

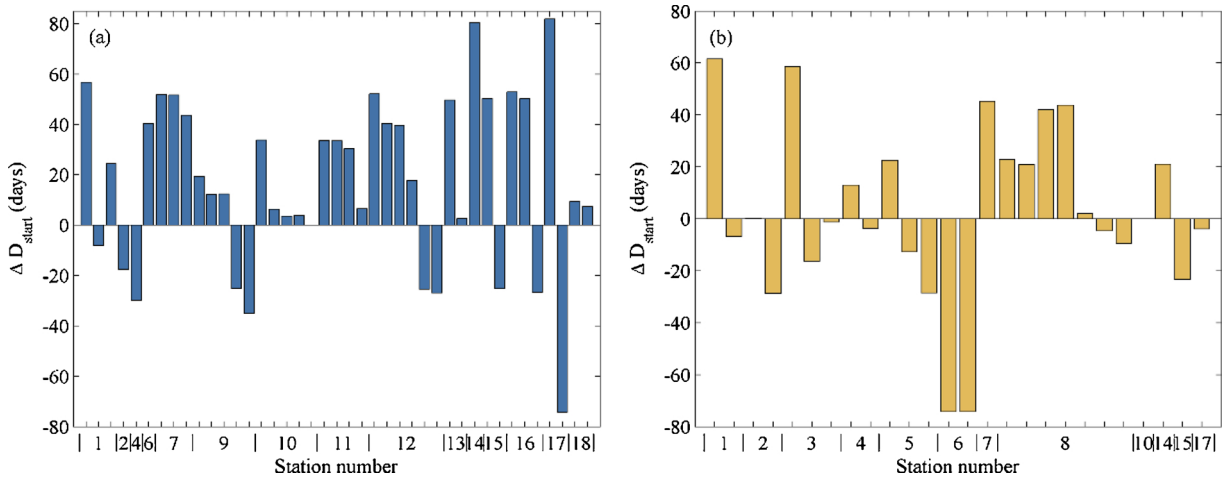

Fig. 3. Differences between D_{start} date of TPMp and average D_{start} date of TPMt. (a) the optimum model TPMp and the non-optimum model TPMt, (b) the optimum model TPMt and the non-optimum model TPMp. Positive value denotes that D_{start} date in TPMp is later than average D_{start} date in TPMt. Negative value means that D_{start} date in TPMp is earlier than average D_{start} date in TPMt.

Specifically, leaf senescence is mainly initiated by photoperiod shortening at 11 stations and by daily minimum temperature decrease at 6 stations (Fig. 5). Moreover, climatic controls on the start of leaf senescence processes depend on annual maximum daylength of the stations. Photoperiod control of leaf senescence start (TPMp) occurs predominantly at stations with shorter annual maximum daylength (32 of 36 time series, 88.9%), while daily minimum temperature control of leaf senescence start (TPMt) appears mainly at stations with longer annual maximum daylength (22 of 31 time series, 71.0%). The transitional photoperiod threshold is around 14.5 h (Fig. 5). Meanwhile, climatic controls on the start of leaf senescence processes are also species-specific to some extent. We note that leaf senescence start for all exotic species (Editorial Board of Flora of China CAS, 1959-2004; Editorial Board of Flora of China CAS, 1959, http://frps.iplant.cn) was predominantly triggered by photoperiod shortening regardless of stations (except for *Populus lasiocarpa* at Huzhu station). In contrast, leaf senescence start for native species (Editorial Board of Flora of China CAS, 1959-2004; Editorial Board of Flora of China CAS, 1959, http://

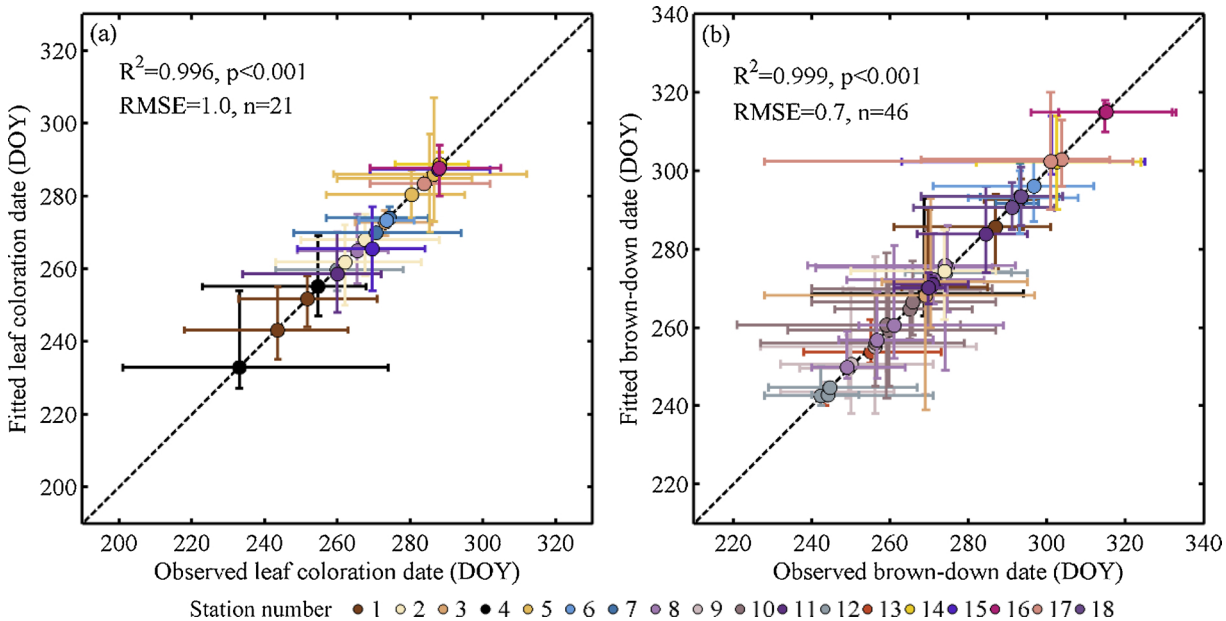

Fig. 4. Comparison between the average (dots) and range (error bars) of fitted and observed senescence dates for woody (a) and herbaceous (b) plants at all stations over 1981–2012. Different color dots denote different stations.

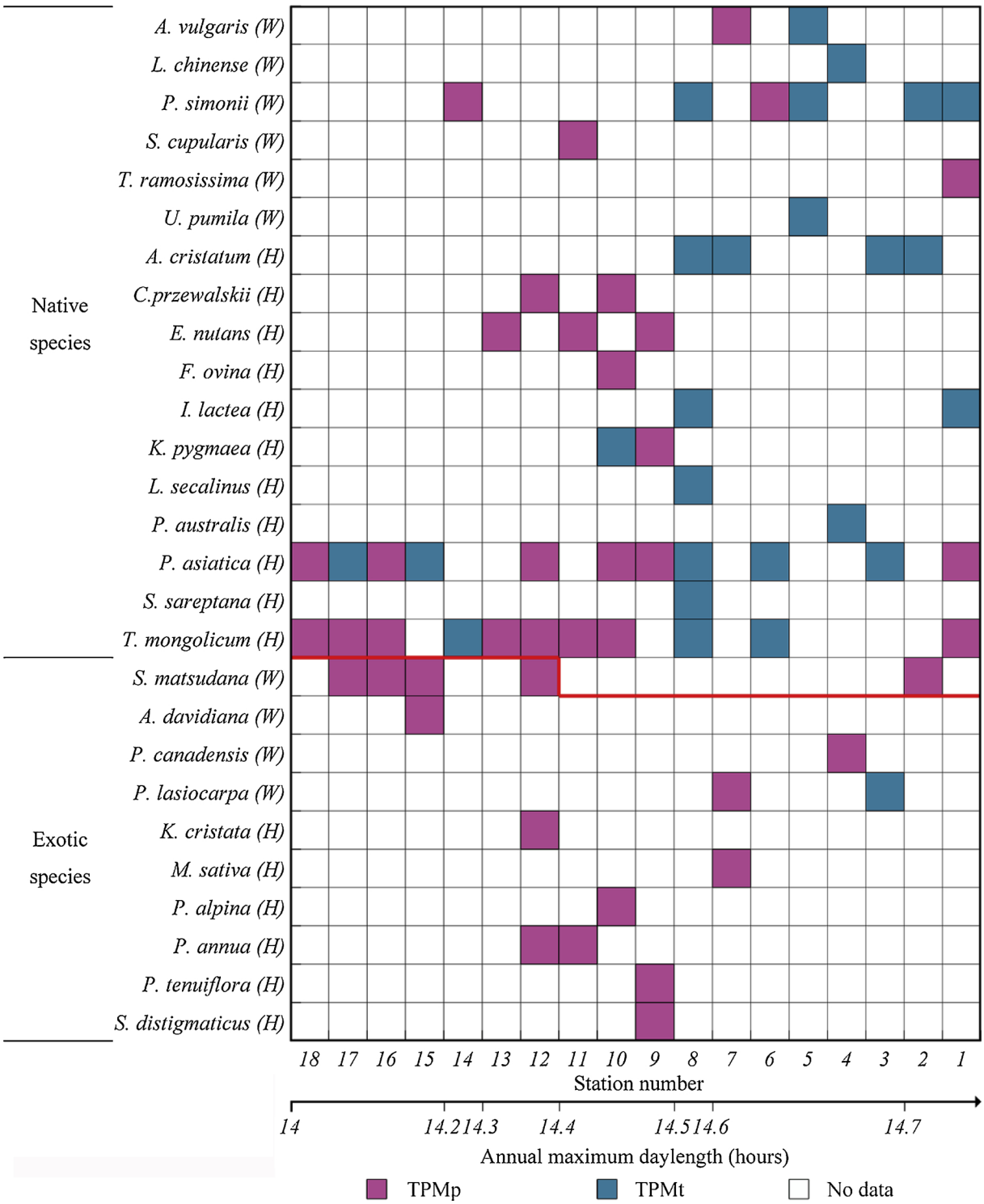

Fig. 5. Dependence of optimum autumn leaf phenology models on annual maximum daylength of the stations and type of the species. The upper bottom horizontal axis labels correspond to the station number, and lower bottom horizontal axis labels correspond to annual maximum daylength of the stations. The vertical axis labels denote different plant species divided into exotic (below the red line) and native (above the red line) species, in which W and H in bracket represent woody plants and herbaceous plants, respectively (For interpretation of the references to colour in this figure legend, the reader is referred to the web version of this article).

frps.iplant.cn) can be induced by photoperiod shortening or minimum temperature decrease (Fig. 5).

3.3. Comparison of TPM, DM and SIAM models in fitting and validation accuracy

To compare the accuracy of our new model (TPM) with existing models, such as DM (Delpierre et al., 2009b) and SIAM (Keenan and Richardson, 2015), we employed DM and SIAM to fit 66 leaf coloration and brown-down time series, respectively. For the latter, corresponding first leaf unfolding time series for woody plants and green-up time series for herbaceous plants were also used. As the DM model has two forms (DM1 having lengthening photoperiod promoting leaf senescence and DM2 having shortening photoperiod promoting leaf senescence;

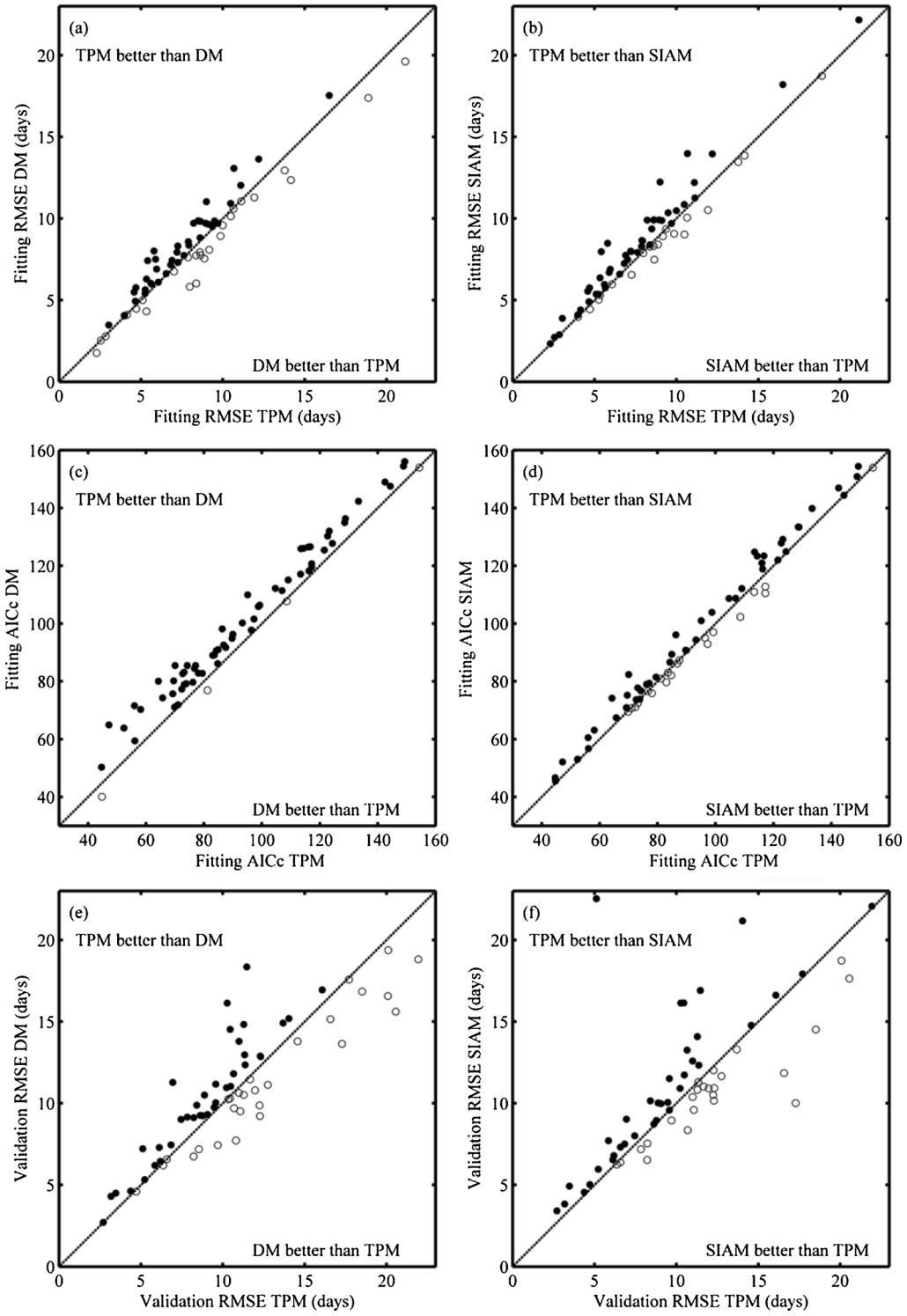

Fig. 6. Comparison of fitting performances among the TPM, DM and SIAM models. (a) fitting RMSE between the TPM and DM models, (b) fitting RMSE between the TPM and SIAM models, (c) fitting AICc between the TPM and DM models, (d) fitting AICc between the TPM and SIAM models, (e) validation RMSE between the TPM and DM models, (f) validation RMSE between the TPM and SIAM models.

Appendix B), we fitted both sub-models and selected the best model based on the smaller RMSE value for each time series. Results show that fitting error (RMSE) of TPM is smaller than those of DM and SIAM in 60.6% and 69.7% of total time series, respectively (Fig. 6a, b), while fitting parsimony and efficiency of TPM are higher (i.e. lower AICc) than those of DM and SIAM in 93.9% and 69.7% of total time series, respectively (Fig. 6c, d). The average fitting RMSE of TPM is 0.2 days and 0.5 days smaller than those of DM and SIAM, while average fitting AICc of TPM is 6.6 and 2.1 smaller than those of DM and SIAM. Similar improvements were also detected in average NSE, namely, average fitting NSE of TPM is 0.28, which is 0.03 and 0.08 larger than those of DM and SIAM. In addition, the average correlation coefficient between fitted and observed leaf coloration/brown-down dates for the TPM model is higher than those for the DM and SIAM models, in which significant correlation coefficients account for 66.7% ($p < 0.05$) and 50% ($p < 0.01$) of total time series for the TPM model. This percentage

Table 3
Comparison of mean correlation coefficient between fitted and observed leaf coloration/brown-down dates among the TPM, DM and SIAM models and significant correlation coefficient in number of time series and its percentage (n = 66).

Model	Average correlation coefficient	Number of time series ($p < 0.05$)	Percentage of time series (%) ($p < 0.05$)	Number of time series ($p < 0.01$)	Percentage of time series (%) ($p < 0.01$)
TPM	0.55	44	66.7	33	50.0
DM	0.50	36	54.5	22	33.3
SIAM	0.46	30	45.5	17	25.8

of time series with significant correlation for the TPM model is also higher than those for the DM and SIAM models (Table 3).

Comparing the new model with the two existing models in validation accuracy, we found that validation error (RMSE) of TPM is smaller than those of DM and SIAM in 57.6% and 63.6% of total time series, respectively (Fig. 6e, f). The average validation RMSE of TPM is 0.3 days and 1.9 days smaller than those of DM and SIAM, respectively. This indicates that the TPM model is more robust than the DM and SIAM models in predicting autumn leaf phenology outside the fitting period.

4. Discussion

4.1. Attributions of spatial and interspecific differentiation of driving factors

This study shows that leaf senescence processes were mainly triggered by photoperiod shortening at locations with shorter annual maximum photoperiod but by night temperature decrease at locations with longer annual maximum photoperiod, especially for the native species (Fig. 5). This finding is supported by numerous experimental photoperiod and temperature treatments (Heide and Prestrud, 2005; Svendsen et al., 2007; Allona et al., 2008; Kalcsits et al., 2009; Horvath et al., 2010). Tanino et al. (2010) summarized two distinct growth cessation pathways of woody plants. One is low night temperature-induced growth cessation under long photoperiods; the other is short photoperiod-induced growth cessation under warm night temperatures. The two pathways reflect plant selective responses to environmental cues for minimizing risk from abiotic stresses. Although growth cessation (or bud set) and autumn senescence are two independent stages, senescence could not be initiated until a certain time after growth cessation (or bud set). This suggests that growth cessation and bud set are important for the trees to acquire competence to respond to the photoperiodic trigger to undergo autumn senescence (Fracheboud et al., 2009; Michelson et al., 2018). In areas with longer annual maximum photoperiods (i.e. northern sites), the need for short photoperiods to cease plant growth is met later before the autumnal equinox (Rohde et al., 2011), while lower temperature constrains photosynthesis and production of chlorophyll (Addicott, 1968; Koike, 1990; Rosenthal and Camm, 1996; Körner, 1998; Worrall, 1998; Zheng et al., 2009; Matos et al., 2012; Archetti et al., 2013). Thus, lower temperature induces the start of leaf senescence process. Contrarily, in areas with shorter annual maximum photoperiods (i.e. southern sites), short photoperiod requirements for plant growth cessation are met earlier before the autumnal equinox (Rohde et al., 2011). Therefore, although the temperature may still be relatively high, leaf senescence process can launch as the photoperiod reaches a threshold.

For all exotic species however, leaf senescence processes were mostly triggered by solely shortening photoperiod regardless of locations. This result is different from insensitive response of exotic species spring phenology to photoperiod (Körner and Basler, 2010). Further experimental studies need to be carried out to explain the physiological and ecological mechanism of this phenomenon.

4.2. Comparison of mechanisms among different models

Besides accuracy, reality and generality are also important criteria for evaluating the effectiveness of a biological model (Levin, 1968). The reality and generality of a model can be interpreted as reasonability of mechanisms behind the model and the unified form of the model. Other than the above mentioned two process-based autumn phenology models (Delpierre et al., 2009b; Keenan and Richardson, 2015), the new model (TPM) predicts leaf senescence process by means of daily minimum temperature instead of daily mean temperature. This is mainly based on the evidence that the minimum temperature may trigger leaf senescence through decreasing light-saturated photosynthetic rate (Zheng et al., 2009; Matos et al., 2012) and limiting meristematic activity in shoot (Körner, 1998). For the latter, as leaf senescence should be intimately related to the previous developmental stages of leaf, such as leaf initiation, growth, and maturation, it is possible that genes controlling these processes, including meristematic activity, could influence age-dependent senescence (Lim et al., 2007). Enhancing meristematic activity in leaves can prolong life span or delay leaf senescence (Ha et al., 2003).

The TPM model revealed coupling effects of shortened photoperiod and decreased daily minimum temperature on leaf senescence processes, namely, as arithmetic product of photoperiod and night air temperature decreases, leaf senescence rate increases. As photoperiod decreases monotonously from summer solstice to winter solstice and remains unchanged across years at a given location, it offers the environmental background of interannual variation of leaf senescence timing. The multiplication relation of daily photoperiod and minimum temperature can reflect not only the decreasing tendency of both photoperiod and temperature during autumn but also the regulation effect of monotonously declining photoperiod on interannually varying temperature at any time points. Further analysis shows that the relative role of night temperature and photoperiod on R_{sen} show a consistent feature in TPMp and TPMt. That is, at the initial stage, the sensitivities of R_{sen} to temperature (partial derivative of R_{sen} with respect to temperature) and photoperiod (partial derivative of R_{sen} with respect to photoperiod) increase steadily with decrease of the arithmetic product of temperature and daylength until reaching the maximum. Then, they decreases along with decrease of the arithmetic product of temperature and daylength. At last, the sensitivities of R_{sen} to temperature and photoperiod achieve the minimum as the leaf senescence rate reaches the maximum. However, the sensitivities of R_{sen} to temperature and photoperiod in the optimum model usually show more typical characteristics with the three stages than those in the corresponding non-optimum model for the same time series (Fig. A1a, b). This is also reflected in differences between the steep exponential curve of R_{sen} for the optimum model and the gentle exponential curve of R_{sen} for the corresponding non-optimum model (Embedded small figure in Fig. A.1a, b). Therefore, the optimum model selected by the lower RMSE can more accurately and effectively portray responses of daily leaf senescence rate to temperature and photoperiod than the non-optimum model, as well as the underlying differential ecological role of temperature and photoperiod during senescence.

By contrast, the DM model shows regulation effect of monotonously declining photoperiod on interannually varying temperature only when

$x \neq 0$ and $y \neq 0$ [Eq. (B.2)]. In other cases ($x = 0$ and $y = 0$; $x = 0$ and $y \neq 0$; $x \neq 0$ and $y = 0$), either temperature or photoperiod controls the leaf senescence process individually, when daily average temperature is lower than a threshold value ($T(d) < T_b$, Eq. (B2); Delpierre et al., 2009b).

Moreover, for the TPM model, leaf senescence can be started when either photoperiod or minimum temperature achieves a threshold, whereas for the DM model, leaf senescence can be launched only when both photoperiod and daily average temperature achieve their thresholds. Our study indicates that leaf senescence processes are triggered by shortened photoperiod rather than lowed night-time temperature at most stations (61.2% of total), which is consistent with previous studies (Worrall, 1998; Larcher, 2003; Körner and Basler, 2010).

Last but not least, our model assumes that leaf senescence is a continuous process and daily leaf senescence rate has saturability. The continuity of leaf senescence means that higher daily minimum temperatures (after the first day when daily minimum temperature is lower than T_{start}) can also promote leaf senescence but in lower rates (R_{sen}) to ensure uninterrupted accumulation of leaf senescence state (S_{sen}). The saturation nature of leaf senescence rate depends on the unified exponential function of the arithmetic product of daily minimum temperature and photoperiod (Fig. 2). Namely, when the arithmetic product of temperature and photoperiod is smaller than a threshold, leaf senescence rate will reach the maximum, so that to enable the leaf senescence to be a stable change process. This may avoid a too early prediction of leaf coloration/brown-down date due to effect of a few very cold nights.

Regarding the SIAM model, the lower accuracy and efficiency is likely caused by less significantly positive correlation between leaf unfolding/green-up date and leaf coloration/brown-down date in the research region (Fig. A.2). A correlation analysis shows that autumn phenological date correlates significantly positive ($p < 0.05$) with spring phenological date only in 15% of total time series (10 of 66 time series) (Fig.A.2), which is consistent with the statistical relationship between first leaf unfolding date and first leaf coloration date in China's temperate zone (Liu et al., 2018).

5. Conclusions

In this study, we developed a new process-based autumn phenology model to simulate and predict leaf coloration and brown-down dates of woody and herbaceous plants on the Qinghai–Tibetan Plateau. Unlike existing models, the new model shows that leaf senescence rate exponentially increases with decrease of arithmetic product of daily minimum temperature and photoperiod. Moreover, driving factors of leaf senescence have significant spatial and interspecific dependence. Photoperiod control of leaf senescence start occurs predominantly at stations with shorter annual maximum daylength, while daily minimum temperature control of leaf senescence start appears mainly at stations with longer annual maximum daylength. Meanwhile, leaf senescence start for all exotic species was predominantly triggered by photoperiod shortening regardless of stations, whereas leaf senescence start for native species can be induced by photoperiod shortening or minimum temperature decrease. Compared with the representative existing process-based autumn phenology models, the new model is a more general model and more robust in fitting and predicting leaf coloration and brown-down dates. Our study has provided a new insight on the understanding of leaf senescence mechanisms in winter deciduous trees and herbaceous plants, and significantly improved the ability to predict climate change impacts on vegetation growth and carbon balance in the world's highest plateau.

Declarations of interest

None.

Acknowledgements

This work was funded by the National Natural Science Foundation of China [grant numbers 41471033, 41771049]. The authors are thankful to Dr. Nicolas Delpierre at the Université Paris-Sud, for reviewing and editing the manuscript. We also thank the Meteorological Information Center of the China Meteorological Administration for providing phenological data.

Appendix A. Supplementary data

Supplementary material related to this article can be found, in the online version, at doi:https://doi.org/10.1016/j.agrformet.2019.01.006.

References

Addicott, F.T., 1968. Environmental factors in physiology of abscission. Plant Physiol. 43, 1471.
Allona, I., Ramos, A., Ibanez, C., Contreras, A., Casado, R., Aragoncillo, C., 2008. Molecular control of winter dormancy establishment in trees. Span. J. Agric. Res. 6, 201–210. https://doi.org/10.5424/sjar/200806S1-389.
Archetti, M., Richardson, A.D., O'Keefe, J., Delpierre, N., 2013. Predicting climate change impacts on the amount and duration of autumn colors in a New England forest. PLoS One 8https://doi.org/10.1371/journal.pone.0057373. e57373.
Baldocchi, D.D., Wilson, K.B., 2001. Modeling CO2 and water vapor exchange of a temperate broadleaved forest across hourly to decadal time scales. Ecol. Modell. 142, 155–184. https://doi.org/10.1016/s0304-3800(01)00287-3.
Baldocchi, D.D., Wong, S., 2008. Accumulated winter chill is decreasing in the fruit growing regions of California. Clim. Change 87, S153–S166. https://doi.org/10.1007/s10584-007-9367-8.
Barr, A.G., Black, T.A., Hogg, E.H., Kljun, N., Morgenstern, K., Nesic, Z., 2004. Inter-annual variability in the leaf area index of a boreal aspen-hazelnut forest in relation to net ecosystem production. Agric. For. Meteorol. 126, 237–255. https://doi.org/10.1016/j.agrformet.2004.06.011.
Barr, A.G., Black, T.A., McCaughey, H., 2009. Climatic and phenological controls of the carbon and energy balances of Three contrasting boreal Forest ecosystems in Western Canada. In: Noormets, A. (Ed.), Phenology of Ecosystem Processes. Springer, Dordrecht, the Netherlands, Heidelberg, New York, London, pp. 3–34.
Black, T.A., Chen, W.J., Barr, A.G., Arain, M.A., Chen, Z., Nesic, Z., Hogg, E.H., Neumann, H.H., Yang, P.C., 2000. Increased carbon sequestration by a boreal deciduous forest in years with a warm spring. Geophys. Res. Lett. 27, 1271–1274. https://doi.org/10.1029/1999gl011234.
Cannell, M.G.R., Smith, R.I., 1983. Thermal time, chill days and prediction of budburst in *Picea sitchensis*. J. Appl. Ecol. 20, 951–963. https://doi.org/10.2307/2403139.
Chen, X., 2013. East Asia. In: Schwartz, M.D. (Ed.), Phenology: An Integrative Environmental Science, 2nd ed. Springer, Dordrecht, the Netherlands, Heidelberg, New York, London, pp. pp. 9–21.
Chen, X., 2017. Spatiotemporal Processes of Plant Phenology: Simulation and Prediction. Springer, Berlin, German.
Chen, H., Zhu, Q., Peng, C., Wu, N., Wang, Y., Fang, X., Gao, Y., Zhu, D., Yang, G., Tian, J., Kang, X., Piao, S., Ouyang, H., Xiang, W., Luo, Z., Jiang, H., Song, X., Zhang, Y., Yu, G., Zhao, X., Gong, P., Yao, T., Wu, J., 2013. The impacts of climate change and human activities on biogeochemical cycles on the Qinghai-Tibetan Plateau. Glob. Change Biol. 19, 2940–2955. https://doi.org/10.1111/gcb.12277.
Chen, X., An, S., Inouye, D.W., Schwartz, M.D., 2015. Temperature and snowfall trigger alpine vegetation green-up on the world's roof. Glob. Change Biol. 21, 3635–3646. https://doi.org/10.1111/gcb.12954.
China Meterological Administration (Ed.), 1993. Observation Criterion of Agicultural Meteorology. China Meterological Press, Beijing, China, pp. pp. 131–164 (in Chinese).
Chuine, I., 2000. A unified model for budburst of trees. J. Theor. Biol. 207, 337–347. https://doi.org/10.1006/jtbi.2000.2178.
Chuine, I., Cour, P., Rousseau, D.D., 1998. Fitting models predicting dates of flowering of temperate-zone trees using simulated annealing. Plant Cell Environ. 21, 455–466. https://doi.org/10.1046/j.1365-3040.1998.00299.x.
Churkina, G., Schimel, D., Braswell, B.H., Xiao, X.M., 2005. Spatial analysis of growing season length control over net ecosystem exchange. Glob. Change Biol. 11, 1777–1787. https://doi.org/10.1111/j.1365-2486.2005.001012.x.
Delpierre, N., Soudani, K., Francois, C., Köstner, B., Pontailler, J.Y., Nikinmaa, E., Misson, L., Aubinet, M., Bernhofer, C., Granier, A., Grunwald, T., Heinesch, B., Longdoz, B., Ourcival, J.M., Rambal, S., Vesala, T., Dufrene, E., 2009a. Exceptional carbon uptake in European forests during the warm spring of 2007: a data–model analysis. Glob. Change Biol. 15, 1455–1474. https://doi.org/10.1111/j.1365-2486.2008.01835.x.
Delpierre, N., Dufrêne, E., Soudani, K., Ulrich, E., Cecchini, S., Boe, J., Francois, C., 2009b. Modelling interannual and spatial variability of leaf senescence for three deciduous tree species in France. Agric. For. Meteorol. 149, 938–948. https://doi.org/10.1016/j.agrformet.2008.11.014.
Dragoni, D., Schmid, H.P., Wayson, C.A., Potter, H., Grimmond, C.S.B., Randolph, J.C., 2011. Evidence of increased net ecosystem productivity associated with a longer

vegetated season in a deciduous forest in south-central Indiana, USA. Glob. Change Biol. 17, 886–897. https://doi.org/10.1111/j.1365-2486.2010.02281.x.
Dufrêne, E., Davi, H., François, C., Maire, Gl., Dantec, V.L., Granier, A., 2005. Modelling carbon and water cycles in a beech forest. Ecol. Modell. 185, 407–436. https://doi.org/10.1016/j.ecolmodel.2005.01.004.
Editorial Board of Flora of China CAS, Flora of China (in Chinese), 1959-2004, Science Press; Beijing, China.
Editorial Board of Vegetation Map of China CAS, 2001. In: Hou, X. (Ed.), 1:1,000,000 Vegetation Atlas of China (in Chinese). Science Press, Beijing, China.
Estiarte, M., Peñuelas, J., 2015. Alteration of the phenology of leaf senescence and fall in winter deciduous species by climate change: effects on nutrient proficiency. Glob. Change Biol. 21, 1005–1017. https://doi.org/10.1111/gcb.12804.
Forsythe, W.C., Rykiel, E.J., Stahl, R.S., Wu, H.I., Schoolfield, R.M., 1995. A model comparison for daylength as a function of latitude and day of year. Ecol. Modell. 80, 87–95. https://doi.org/10.1016/0304-3800(94)00034-f.
Fracheboud, Y., Luquez, V., Bjorken, L., Sjodin, A., Tuominen, H., Jansson, S., 2009. The control of autumn senescence in european Aspen. Plant Physiol. 149, 1982–1991. https://doi.org/10.1104/pp.108.133249.
Fu, Y.H., Campioli, M., Demaree, G., Deckmyn, A., Hamdi, R., Janssens, I.A., Deckmyn, G., 2012. Bayesian calibration of the Unified budburst model in six temperate tree species. Int. J. Biometeorol. 56, 153–164. https://doi.org/10.1007/s00484-011-0408-7.
Fu, Y.S., Campioli, M., Vitasse, Y., De Boeck, H.J., Van den Berge, J., AbdElgawad, H., Asard, H., Piao, S.L., Deckmyn, G., Janssens, I.A., 2014. Variation in leaf flushing date influences autumnal senescence and next year's flushing date in two temperate tree species. Proc. Natl. Acad. Sci. U. S. A. 111, 7355–7360. https://doi.org/10.1073/pnas.1321727111.
Goulden, M.L., Munger, J.W., Fan, S.M., Daube, B.C., Wofsy, S.C., 1996. Exchange of carbon dioxide by a deciduous forest: response to interannual climate variability. Science 271, 1576–1578. https://doi.org/10.1126/science.271.5255.1576.
Ha, C.M., Kim, G.T., Kim, B.C., Jun, J.H., Soh, M.S., Ueno, Y., Machida, Y., Tsukaya, H., Nam, H.G., 2003. The BLADE-ON-PETIOLE 1 gene controls leaf pattern formation through the modulation of meristematic activity in Arabidopsis. Development 130, 161–172. https://doi.org/10.1242/dev.00196.
Hagen, S.C., Braswell, B.H., Linder, E., Frolking, S., Richardson, A.D., Hollinger, D.Y., 2006. Statistical uncertainty of eddy-flux based estimates of gross ecosystem carbon exchange at Howland Forest, Maine. J. Geophys. Res. D: Atmos. 111, 1–12. https://doi.org/10.1029/2005jd006154.
Hänninen, H., 1990. Modelling bud dormancy release in trees from cool and temperate regions. Acta For. Fenn. 213, 1–47.
Hastie, T., Tibshirani, R., Friedman, J., 2001. The Elements of Statistical Learning: Data Mining, Inference, and Prediction. Springer, NewYork.
Heide, O.M., Prestrud, A.K., 2005. Low temperature, but not photoperiod, controls growth cessation and dormancy induction and release in apple and pear. Tree Physiol. 25, 109–113. https://doi.org/10.1093/treephys/25.1.109.
Hollinger, D., Aber, J., Dail, B., Davidson, E., Goltz, S., Hughes, H., Leclerc, M., Lee, J., Richardson, A., Rodrigues, C., 2004. Spatial and temporal variability in forest-atmosphere CO2 exchange. Glob. Change Biol. 10, 1689–1706. https://doi.org/10.1111/j.1365-2486.2004.00847.x.
Horvath, D.P., Sung, S., Kim, D., Chao, W., Anderson, J., 2010. Characterization, expression and function of DORMANCY ASSOCIATED MADS-BOX genes from leafy spurge. Plant Mol. Biol. 73, 169–179. https://doi.org/10.1007/s11103-009-9596-5.
Hurvich, C.M., Tsai, C.L., 1989. Rgression and time-series model selection in small samples. Biometrika 76, 297–307. https://doi.org/10.2307/2336663.
IPCC, 2013. Summary for policymakers. In. In: Stocker, T.F., Qin, D., Plattner, G.-K., Tignor, M., Allen, S.K., Boschung, J., Nauels, A., Xia, Y., Bex, V., Midgley, P.M. (Eds.), Climate Change 2013: The Physical Science Basis. Contribution of Working Group I to the Fifth Assessment Report of the Intergovernmental Panel on Climate Change. Cambridge University Press, Cambridge, United Kingdom and New York, NY, USA.
Kalcsits, L.A., Silim, S., Tanino, K., 2009. Warm temperature accelerates short photoperiod-induced growth cessation and dormancy induction in hybrid poplar (*Populus* × *spp.*). Trees 23, 971–979. https://doi.org/10.1007/s00468-009-0339-7.
Keeling, C.D., Chin, J.F.S., Whorf, T.P., 1996. Increased activity of northern vegetation inferred from atmospheric CO2 measurements. Nature 382, 146–149. https://doi.org/10.1038/382146a0.
Keenan, T.F., Richardson, A.D., 2015. The timing of autumn senescence is affected by the timing of spring phenology: implications for predictive models. Observ. Criterion Agic. Meteorol. 21, 2634–2641. https://doi.org/10.1111/gcb.12890.
Keenan, T.F., Gray, J., Friedl, M.A., Toomey, M., Bohrer, G., Hollinger, D.Y., Munger, J.W., O'Keefe, J., Schmid, H.P., Wing, I.S., 2014. Net carbon uptake has increased through warming-induced changes in temperate forest phenology. Nat. Clim. Change 4, 598–604. https://doi.org/10.1038/nclimate2253.
Kljun, N., Black, T.A., Griffis, T.J., Barr, A.G., Gaumont-Guay, D., Morgenstern, K., McCaughey, J.H., Nesic, Z., 2007. Response of net ecosystem productivity of three boreal forest stands to drought. Ecosystems 10, 1039–1055. https://doi.org/10.1007/s10021-007-9088-x.
Kobayashi, K.D., Fuchigami, L.H., English, M.J., 1982. Modeling temperature requirements for rest development in *Cornus sericea*. J. Am. Soc. Hortic. Sci. 107, 914–918.
Koike, T., 1990. Autumn coloring, photosynthetic performance and leaf development of deciduous broad-leaved trees in relaiton to forest succession. Tree Physiol. 7, 21–32. https://doi.org/10.1093/treephys/7.1-2-3-4.21.
Körner, C., 1998. A re-assessment of high elevation treeline positions and their explanation. Oecologia 115, 445–459. https://doi.org/10.1007/s004420050540.
Körner, C., Basler, D., 2010. Phenology under global warming. Science 327, 1461–1462. https://doi.org/10.1126/science.1186473.
Kramer, K., 1994. Selecting a model to predict the onset of growth of *Fagus sylvatica*. J. Appl. Ecol. 31, 172–181. https://doi.org/10.2307/2404609.
Landsberg, J.J., 1974. Apple fruit bud development and growth: analysis and an empirical model. Ann. Bot. 38, 1013–1023. https://doi.org/10.1093/oxfordjournals.aob.a084891.
Larcher, W., 2003. Physiological Plant Ecology, 4th ed. Springer-Verlag, Berlin,German.
Levins, R., 1968. Evolution in Changing Environments: Some Theoretical Explorations. Princeton University Press, Princeton, N.J. United States.
Lim, P.O., Kim, H.J., Nam, H.G., 2007. Leaf senescence.*ANnu. Rev.* Plant Biol. 58, 115–136. https://doi.org/10.1146/annurev.arplant.57.032905.105316.
Linkosalo, T., Lappalainen, H.K., Hari, P., 2008. A comparison of phenological models of leaf bud burst and flowering of boreal trees using independent observations. Tree Physiol. 28, 1873–1882. https://doi.org/10.1093/treephys/28.12.1873.
Liu, G., Chen, X., Zhang, Q., Lang, W., Delpierre, N., 2018. Antagonistic effects of growing season and autumn temperatures on the timing of leaf coloration in winter deciduous trees. Glob. Change Biol. Bioenergy 24, 3537–3545. https://doi.org/10.1111/gcb.14095.
Matos, F.S., de Oliveria, L.R., de Freitas, R.G., Evaristo, A.B., Missio, R.F., Cano, M.A.O., Dias, L.A.D., 2012. Physiological characterization of leaf senescence of *Jatropha curcas L.* Populations. Biomass Bioenergy 45, 57–64. https://doi.org/10.1016/j.biombioe.2012.05.012.
Michelson, I.H., Ingvarsson, P.K., Robinson, K.M., Edlund, E., Eriksson, M.E., Nilsson, O., Jansson, S., 2018. Autumn senescence in aspen is not triggered by day length. Physiol. Plant. 162, 123–134. https://doi.org/10.1111/ppl.12593.
Morin, X., Lechowicz, M.J., Augspurger, C., O' Keefe, J., Viner, D., Chuine, I., 2009. Leaf phenology in 22 North American tree species during the 21st century. Glob. Change Biol. Bioenergy 15, 961–975. https://doi.org/10.1111/j.1365-2486.2008.01735.x.
Murray, C, M.G.R., S, R.I., 1989. Date of budburst of fifteen tree species in Britain following climatic warming. J. Appl. Ecol. 26, 693–700. https://doi.org/10.2307/2404093.
Myneni, R.B., Keeling, C.D., Tucker, C.J., Asrar, G., Nemani, R.R., 1997. Increased plant growth in the northern high latitudes from 1981 to 1991. Nature 386, 698–702. https://doi.org/10.1038/386698a0.
Nash, J.E., Sutcliffe, J.V., 1970. River flow forecasting through conceptual models part I — a discussion of principles. J. Hydrol. (Amst) 10, 282–290. https://doi.org/10.1016/0022-1694(70)90255-6.
Peñuelas, J., Rutishauser, T., Filella, I., 2009. Phenology feedbacks on climate change. Science 324, 887–888. https://doi.org/10.1126/science.1173004.
Pudas, E., Tolvanen, A., Poikolainen, J., Sukuvaara, T., Kubin, E., 2008. Timing of plant phenophases in Finnish Lapland in 1997-2006. Boreal Environ. Res. 13, 31–43.
Richardson, A.D., O'Keefe, J., 2009. Phenological differences between understory and overstory: a case dtudy using the long-term Harvard forest records. In: Noormets, A. (Ed.), Phenology of Ecosystem Processes. Springer, Dordrecht, the Netherlands, Heidelberg, New York, London, pp. pp. 87–117.
Richardson, A.D., Black, T.A., Ciais, P., Delbart, N., Friedl, M.A., Gobron, N., Hollinger, D.Y., Kutsch, W.L., Longdoz, B., Luyssaert, S., 2010. Influence of spring and autumn phenological transitions on forest ecosystem productivity. Philos. Trans. R. Soc. London, Ser. B 365, 3227–3246. https://doi.org/10.1098/rstb.2010.0102.
Richardson, A.D., Keenan, T.F., Migliavacca, M., Ryu, Y., Sonnentag, O., Toomey, M., 2013. Climate change, phenology, and phenological control of vegetation feedbacks to the climate system. Agric. For. Meteorol. 169, 156–173. https://doi.org/10.1016/j.agrformet.2012.09.012.
Rohde, A., Bastien, C., Boerjan, W., 2011. Temperature signals contribute to the timing of photoperiodic growth cessation and bud set in poplar. Tree Physiol. 31, 472–482. https://doi.org/10.1093/treephys/tpr038.
Rosenthal, S.I., Camm, E.L., 1996. Effects of air temperature, photoperiod and leaf age on foliar senescence of western larch (*Larix occidentalis Nutt*) in environmentally controlled chambers. Plant Cell Environ. 19, 1057–1065. https://doi.org/10.1111/j.1365-3040.1996.tb00212.x.
Schwartz, M.D., 1996. An air mass-based approach to regional GCM validation. Clim. Res. 6, 227–235. https://doi.org/10.3354/cr006227.
Soolanayakanahally, R.Y., Guy, R.D., Silim, S.N., Song, M.H., 2013. Timing of photoperiodic competency causes phenological mismatch in balsam poplar (*Populus balsamifera L.*). Plant Cell Environ. 36, 116–127. https://doi.org/10.1111/j.1365-3040.2012.02560.x.
Svendsen, E., Wilen, R., Stevenson, R., Liu, R.S., Tanino, K.K., 2007. A molecular marker associated with low-temperature induction of dormancy in red osier dogwood (*Cornus sericea*). Tree Physiol. 27, 385–397. https://doi.org/10.1093/treephys/27.3.385.
Tanino, K.K., Kalcsits, L., Silim, S., Kendall, E., Gray, G.R., 2010. Temperature-driven plasticity in growth cessation and dormancy development in deciduous woody plants: a working hypothesis suggesting how molecular and cellular function is affected by temperature during dormancy induction. Plant Mol. Biol. 73, 49–65. https://doi.org/10.1007/s11103-010-9610-y.
Tao, Z., Wang, H., Dai, J., Alatalo, J., Ge, Q., 2017. Modeling spatiotemporal variations in leaf coloring date of three tree species across China. Agric. For. Meteorol. 249, 310–318. https://doi.org/10.1016/j.agrformet.2017.10.034.
Vegis, A., 1964. Dormancy in higher plants. Annu. Rev. Plant Physiol. 15, 185–224. https://doi.org/10.1146/annurev.pp.15.060164.001153.
Vitasse, Y., François, C., Delpierre, N., Dufrêne, E., Kremer, A., Chuine, I., Delzon, S., 2011. Assessing the effects of climate change on the phenology of European

temperate trees. Agric. For. Meteorol. 151, 969–980. https://doi.org/10.1016/j.agrformet.2011.03.003.
White, M.A., Nemani, A.R., 2003. Canopy duration has little influence on annual carbon storage in the deciduous broad leaf forest. Glob. Change Biol. 9, 967–972. https://doi.org/10.1046/j.1365-2486.2003.00585.x.
Wilson, K.B., Baldocchi, D.D., 2000. Seasonal and interannual variability of energy fluxes over a broadleaved temperate deciduous forest in North America. Agric. For. Meteorol. 100, 1–18. https://doi.org/10.1016/s0168-1923(99)00088-x.
Worrall, J., 1998. Autumn leaf colouration. For. Chron. 74, 668–669.
Wu, C., Chen, J.M., Black, T.A., Price, D.T., Kurz, W.A., Desai, A.R., Gonsamo, A., Jassal, R.S., Gough, C.M., Bohrer, G., 2013. Interannual variability of net ecosystem productivity in forests is explained by carbon flux phenology in autumn. Glob. Ecol. Biogeogr. 22, 994–1006. https://doi.org/10.1111/geb.12044.
Zheng, Y.L., Feng, Y.L., Lei, Y.B., Yang, C.Y., 2009. Different photosynthetic responses to night chilling among twelve populations of Jatropha curcas. Photosynthetica 47, 559–566. https://doi.org/10.1007/s11099-009-0081-9.
Zheng, D., Yang, Q., Wu, S., 2015. Physical Geography of China (in Chinese). Science Press, Beijing, China.